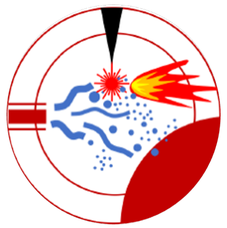
High-Speed Reactive Flow Simulations on Exascale Systems: Applications to Rocket Combustors

Advanced Modeling & Simulation (AMS) Seminar Series
NASA Ames Research Center, May 28th, 2026

*Alboreno Voci**, Diego Rossinelli, Mario Di Renzo

Advisor: Sanjiva Lele, Gianluca Iaccarino (co-advisor)



This material is based upon work supported by the Department of Energy,
National Nuclear Security Administration under Award Number DE-NA0003968
and Los Alamos National Laboratory.





PSAAP III – INSIEME

Physical Challenges

- Cryogenic temperatures
- Flash evaporation
- Multiphase compressible turbulent flow
- Stiff chemistry



First successful Raptor engine relight in space, flight 6[1].

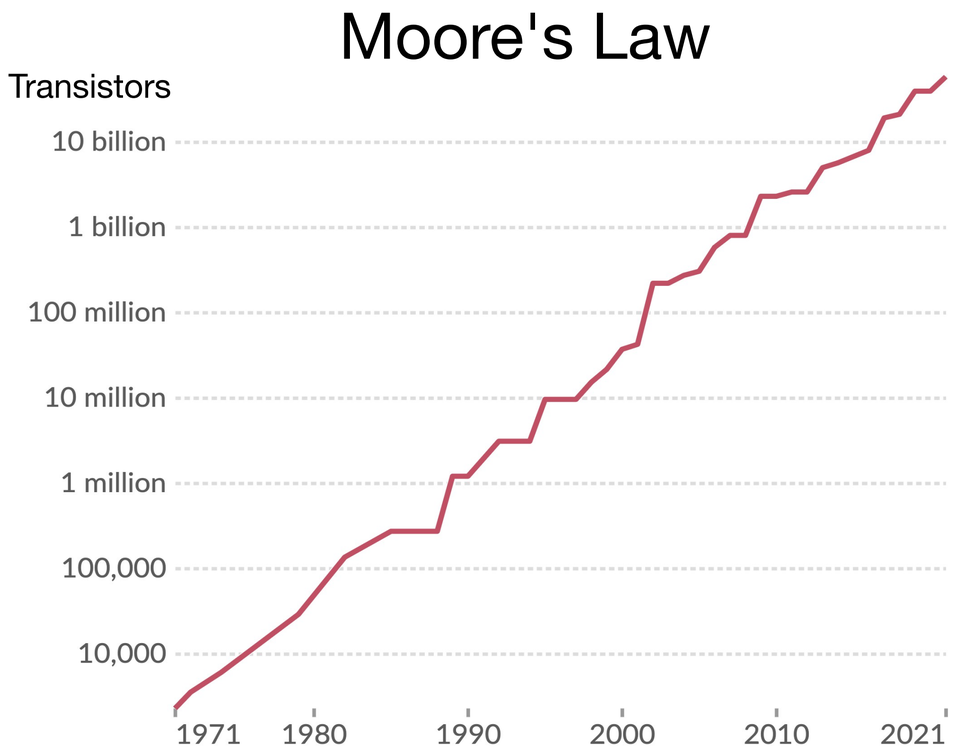
[1]. SpaceX, Starship Flight 6 (2024).

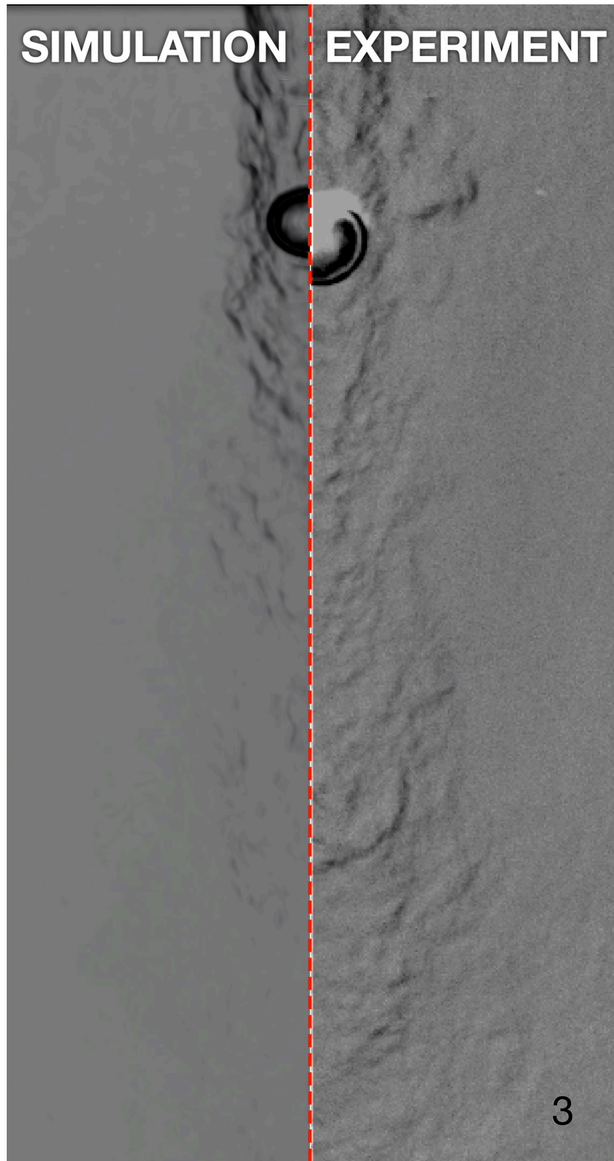
Computational Fluid Dynamics (CFD)

Governing equations: coupled, non-linear PDEs

Contributing factors

- Number of transistors
- Numerical methods





[1]. Rossinelli et al. Gallery of Fluid Motion, American Physical Society (2025).

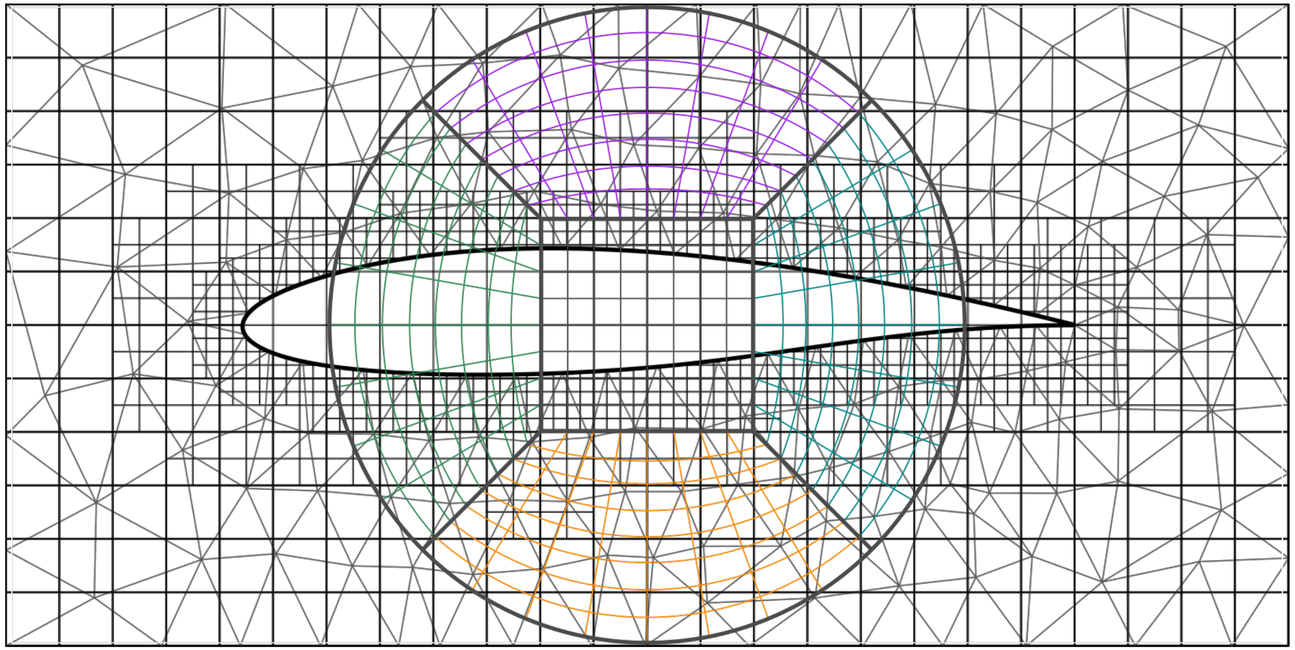
Grids

Mesh quality dictates solution accuracy

- Mesh automation & optimization[1]

Commonly used grids

- Cartesian with immersed boundary
- Unstructured
- Semi-structured
- Structured
- **Structured multiblock**



[1]. Cary, Andrew W., et al. *Cfd vision 2030 road map: Progress and perspectives*. AIAA aviation 2021 forum (2021).

Solver suite

Hypersonics Task-based Research[1] (HTR) solver

- Single block, curvilinear coordinates
- Compressible flow
- Reacting flow
- Multiphase flow

Legion/Regent[2,3] software stack

- Task/data parallelism
- Multi-fidelity ensembles



LLNL Lassen[4] supercomputer.

[1]. Di Renzo et al. *HTR solver: An open-source exascale-oriented task-based multi-GPU high-order code for hypersonic aerothermodynamics*. *CPC* (2020).
[2]. Bauer et al. *Legion: Expressing locality and independence with logical regions*. IEEE (2012).
[3]. Slaughter et al. *Regent: A High-Productivity Programming Language for HPC*. SC '15 (2015).
[4]. Lawrence Livermore National Lab. https://hpc.llnl.gov/hardware/compute-platforms/lassen

Outline

- Introduction
- **Effect of singularities on multiblock grids**
- Legion/Regent software stack
- High Performance Computing
- Applications
- Conclusions

State of the art

Extension of single block implementations

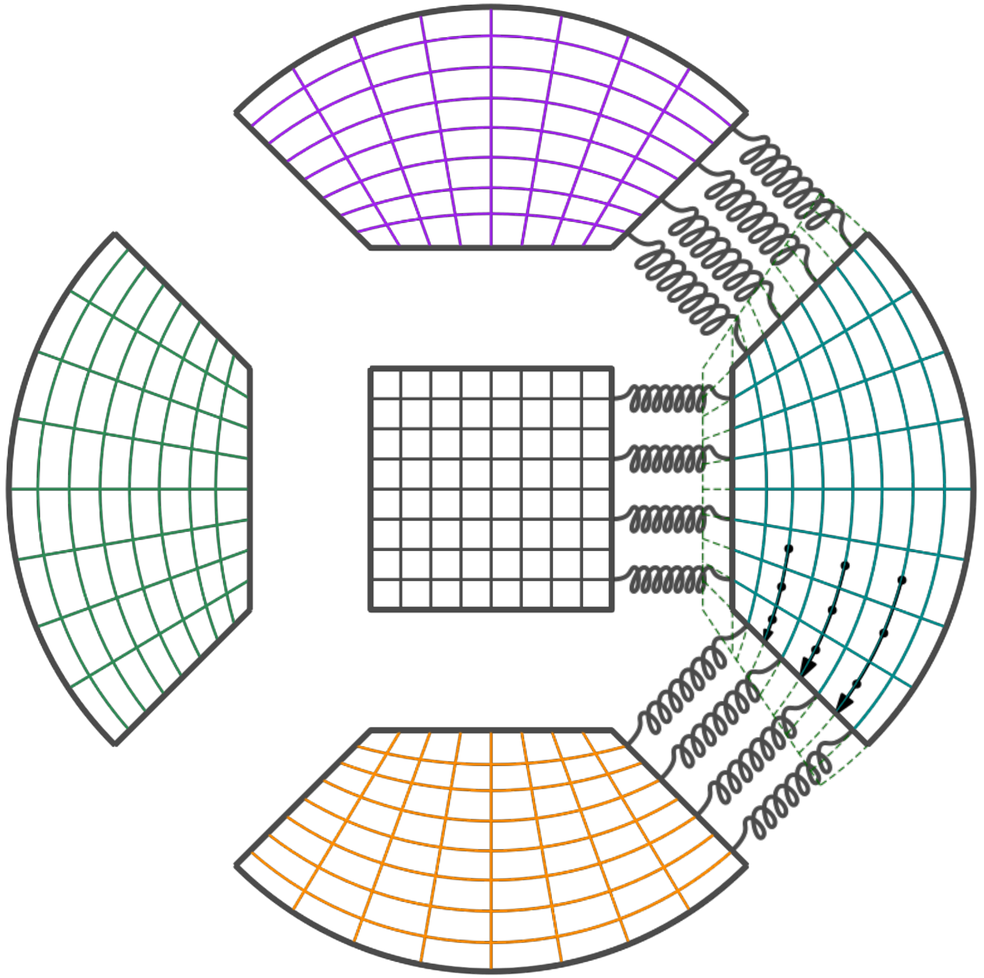
Finite difference applications

- Simultaneous Approximation Term (SAT)[1]
- Ghost interpolation[2]
- One-sided differences[3]

Finite volume applications

- Special case of unstructured grids
- High order implementations[4]

<u>Treatment is necessary at block interfaces</u>



[1]. Nordström et al. *A stable and conservative high order multi-block method for the compressible Navier–Stokes equations*. JCP (2009).
[2]. Chandravamsi et al. *On the application of gradient based reconstruction for flow simulations on generalized curvilinear and dynamic mesh domains*. C&F (2023).
[3]. Wang et al. *On numerical integration and conservation of cell-centered finite difference method*. JSC (2024).
[4]. McCorquodale et al. *High-order finite-volume methods for hyperbolic conservation laws on mapped multiblock grids.* JCP (2015).

Governing equations

Filtered Navier-Stokes (NS) equations

- Large Eddy Simulation (LES) setting
- Diffuse interface method
- 4 equation model formulation[1]
- Finite rate chemistry

Species diffusion

Turbulent spray model[2]

HK phase change model[3]

Chemical production rates

$$\frac{\partial \bar{\rho}\widetilde{Y}_p^c}{\partial t} + \frac{\partial \widetilde{u}_j \bar{\rho}\widetilde{Y}_p^c}{\partial x_j} = -\frac{\partial}{\partial x_j}\left(\overline{J_{p,j}^c} + \overline{J_{p,j}^c}^t + \overline{R_{p,j}^c}\right) + \overline{\dot{m}_p^c} + \overline{\dot{\omega}_p^c}$$

$$\frac{\partial \bar{\rho}\widetilde{u}_i}{\partial t} + \frac{\partial \widetilde{u}_j \bar{\rho}\widetilde{u}_i}{\partial x_j} = -\frac{\partial}{\partial x_j}\left(\overline{P}\delta_{ij} + \overline{\tau_{ij}} + \overline{\tau_{ij}}^t + \widetilde{u}_i\overline{R_j}\right)$$

$$\frac{\partial \bar{\rho}\widetilde{E}}{\partial t} + \frac{\partial \widetilde{u}_j \bar{\rho}\widetilde{E}}{\partial x_j} = -\frac{\partial}{\partial x_j}\left(\overline{P}\widetilde{u}_j + \overline{\tau_{ij}}\widetilde{u}_j + \overline{\tau_{ij}}^t\widetilde{u}_j + \overline{Q_j} + \overline{Q_j}^t + \overline{H_j} + \widetilde{u}_i\widetilde{u}_i\overline{R_j}/2\right)$$

---

[1]. Collis et al. *A thermodynamically consistent and robust four-equation model for multi-phase multi-component ...* . arXiv preprint (2025).
[2]. Lebas et al. *Numerical simulation of primary break-up and atomization: DNS and modelling study.* IJMF (2009).
[3]. Hertz, H. *Uber die Verdunstung der Flüssigkeiten, ins besonderedes Quecksilbers, im luftleeren Raume.* Annalen der Physik (1882).

Governing equations

Filtered Navier-Stokes equations

- Large Eddy Simulation (LES) setting
- Diffuse interface method
- 4 equation model formulation[1]
- Finite rate chemistry

Vector form:

$$\frac{\partial \mathbf{C}}{\partial t} + \frac{\partial \mathbf{F}}{\partial x} + \frac{\partial \mathbf{G}}{\partial y} + \frac{\partial \mathbf{H}}{\partial z} - \frac{\partial \mathbf{F}_v}{\partial x} - \frac{\partial \mathbf{G}_v}{\partial y} - \frac{\partial \mathbf{H}_v}{\partial z} = \dot{\mathbf{S}}$$

Conserved variables | Convective fluxes | Diffusive fluxes | Source terms

[1]. Collis et al. *A thermodynamically consistent and robust four-equation model for multi-phase multi-component ...* . arXiv preprint (2025).
[2]. Lebas et al. *Numerical simulation of primary break-up and atomization: DNS and modelling study.* IJMF (2009).
[3]. Hertz, H. *Uber die Verdunstung der Flüssigkeiten, ins besonderedes Quecksilbers, im luftleeren Raume.* Annalen der Physik (1882).

Curvilinear transformation

Coordinate mapping

$$\mathbb{M} = \begin{bmatrix} \xi_x & \xi_y & \xi_z \\ \eta_x & \eta_y & \eta_z \\ \zeta_x & \zeta_y & \zeta_z \end{bmatrix} = \begin{bmatrix} x_\xi & x_\eta & x_\zeta \\ y_\xi & y_\eta & y_\zeta \\ z_\xi & z_\eta & z_\zeta \end{bmatrix}^{-1}, \quad J = \det(\mathbb{M})$$

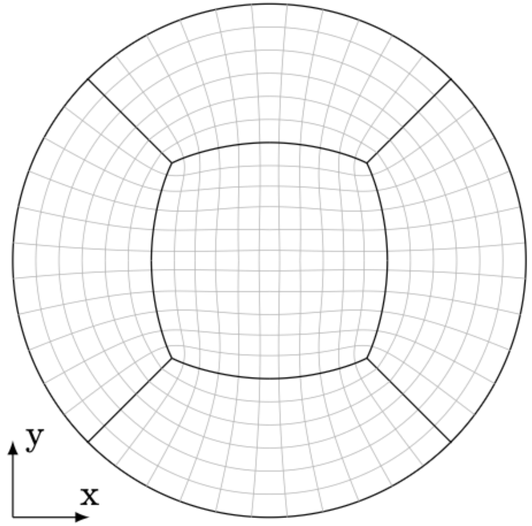
Transformed equations in vector form

$$\frac{\partial \widehat{\mathbf{C}}}{\partial t} + \frac{\partial \widehat{\mathbf{F}}}{\partial \xi} + \frac{\partial \widehat{\mathbf{G}}}{\partial \eta} + \frac{\partial \widehat{\mathbf{H}}}{\partial \zeta} - \frac{\partial \widehat{\mathbf{F}}_v}{\partial \xi} - \frac{\partial \widehat{\mathbf{G}}_v}{\partial \eta} - \frac{\partial \widehat{\mathbf{H}}_v}{\partial \zeta} = \dot{\widehat{\mathbf{S}}}$$

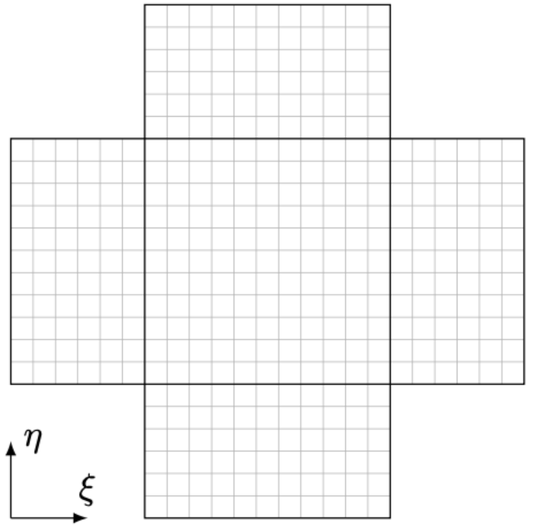
where

$$\widehat{\mathbf{F}} = \frac{\mathbf{F}\xi_x + \mathbf{G}\xi_y + \mathbf{H}\xi_z}{J}$$

Physical space



Reference domain



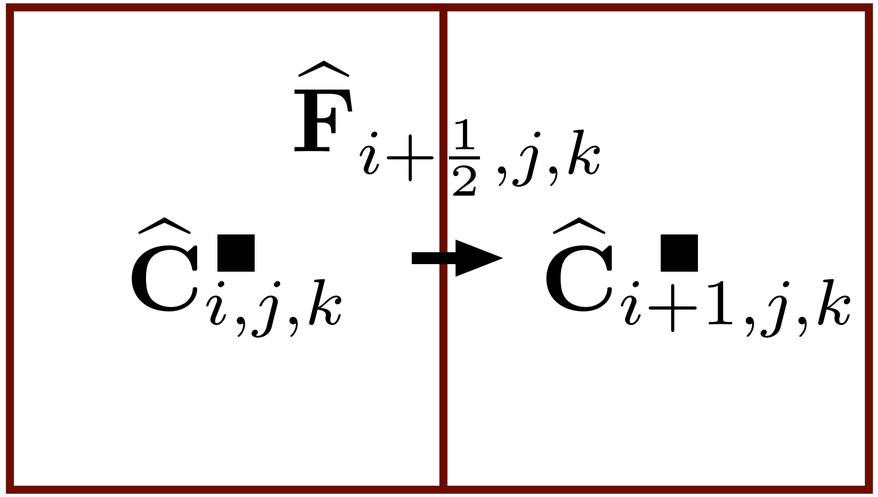
Numerical discretization

Collocated finite difference

Convective fluxes: 6th order

- Skew-symmetric[1]
- TENO/WENO[2,3]

$$\left.\frac{\partial \widehat{\mathbf{F}}}{\partial \xi}\right|_{i,j,k} = \widehat{\mathbf{F}}_{i+\frac{1}{2},j,k} - \widehat{\mathbf{F}}_{i-\frac{1}{2},j,k}$$



Diffusive fluxes: 2nd order

Time stepping scheme: 3rd order SSP-RK

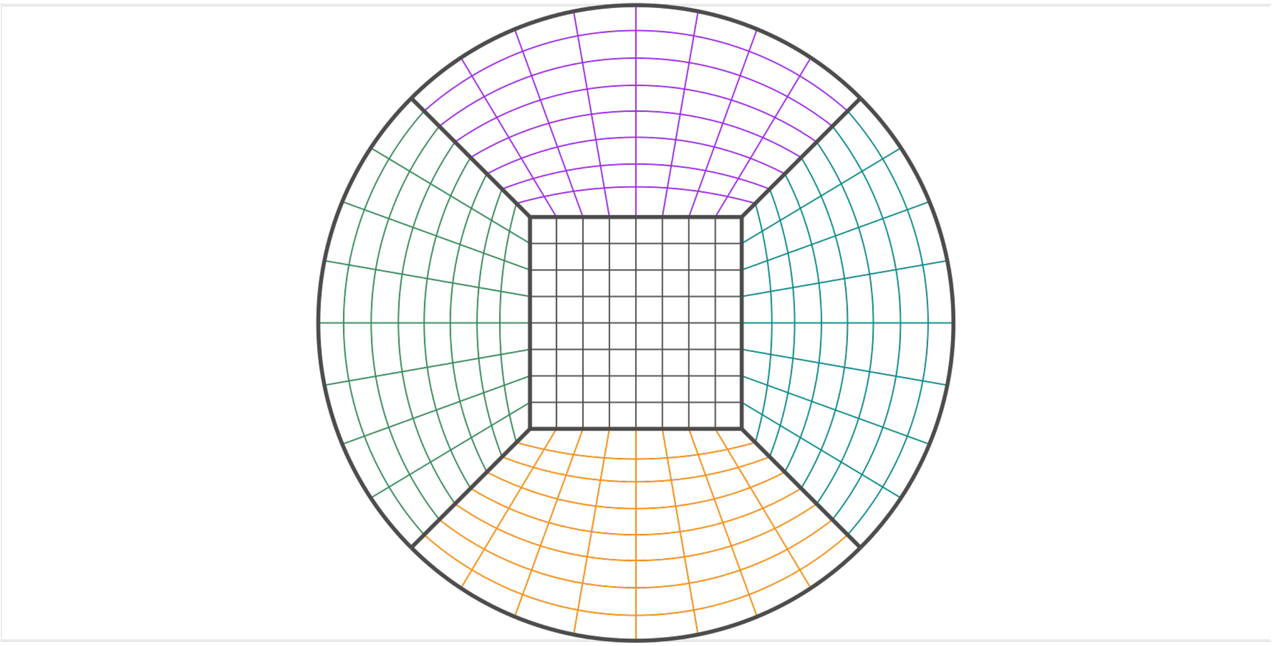
[1]. Pirozzoli, S. *Generalized conservative approximations of split convective derivative operators*. JCP (2010).
[2]. Jiang et al. *Efficient Implementation of Weighted ENO Schemes*. JCP (1996).
[3]. Fu et al. *A family of high-order targeted ENO schemes for compressible-fluid simulations*. JCP (2016).

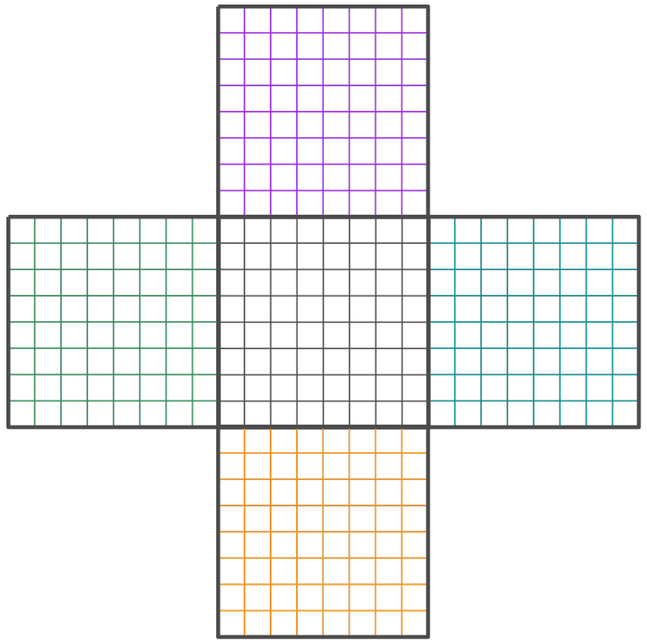
Multiblock grids

Increased flexibility and grid quality

- Automated mesh generation tools[1]
- Custom mesh design

Singularity: lack of a unique mapping



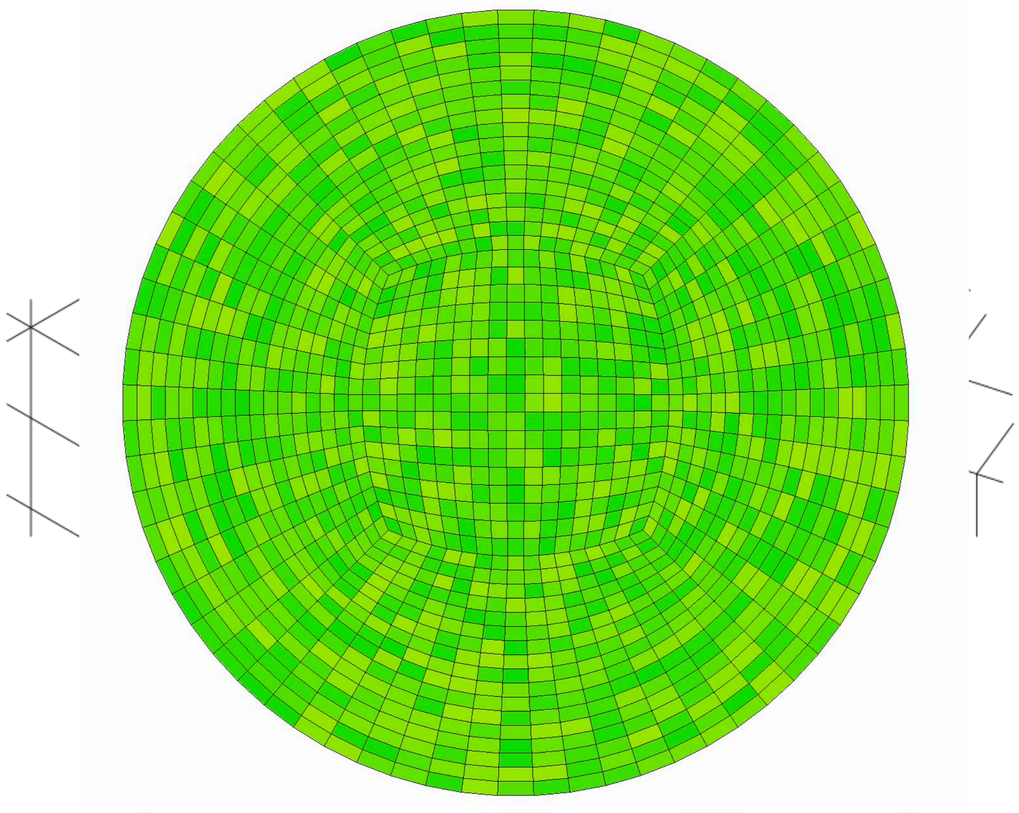


Discretization

Stencils are well defined

- Numerical scheme can be uniformly applied

Constant (equilibrium) state satisfies the NS/LES equations



Numerical error

- The flux term:

$$\widehat{\mathbf{F}} = \frac{\mathbf{F}\xi_x + \mathbf{G}\xi_y + \mathbf{H}\xi_z}{J}$$

- The divergence operator:

$$\left.\frac{\partial \widehat{\mathbf{F}}}{\partial \xi}\right|_{i,j,k} = \widehat{\mathbf{F}}_{i+\frac{1}{2},j,k} - \widehat{\mathbf{F}}_{i-\frac{1}{2},j,k}$$

$$\left.\frac{\partial \widehat{\mathbf{F}}}{\partial \xi}\right|_{i,j,k} = \frac{1}{J}\left[\left.\left(\mathbf{F}\xi_x\right)\right|_{i+\frac{1}{2},j,k} - \left.\left(\mathbf{F}\xi_x\right)\right|_{i-\frac{1}{2},j,k}\right] + \cdots$$

- For a constant state $\mathbf{C}^c$, governing equations reduce to

$$\left.\begin{aligned} I_x &= \frac{\partial}{\partial \xi}\left(\frac{\xi_x}{J}\right) + \frac{\partial}{\partial \eta}\left(\frac{\eta_x}{J}\right) + \frac{\partial}{\partial \zeta}\left(\frac{\zeta_x}{J}\right) = 0 \\ I_y &= \frac{\partial}{\partial \xi}\left(\frac{\xi_y}{J}\right) + \frac{\partial}{\partial \eta}\left(\frac{\eta_y}{J}\right) + \frac{\partial}{\partial \zeta}\left(\frac{\zeta_y}{J}\right) = 0 \\ I_z &= \frac{\partial}{\partial \xi}\left(\frac{\xi_z}{J}\right) + \frac{\partial}{\partial \eta}\left(\frac{\eta_z}{J}\right) + \frac{\partial}{\partial \zeta}\left(\frac{\zeta_z}{J}\right) = 0 \end{aligned}\right\}$$

Geometrical Conservation Law[1]

[1]. Thomas et al. *Geometric Conservation Law and Its Application to Flow Computations on Moving Grids*. AIAA Journal (1979).

Geometric conservation law

2 necessary conditions to satisfy the GCL[1,2]

- Conservative metrics discretization
- Consistent operators for metrics & fluxes
  - Implies discrete derivative operators should commute

$$D^{\xi}(D^{\eta} f) = D^{\eta}(D^{\xi} f)$$

Symmetric Conservative Metrics Method (SCMM)

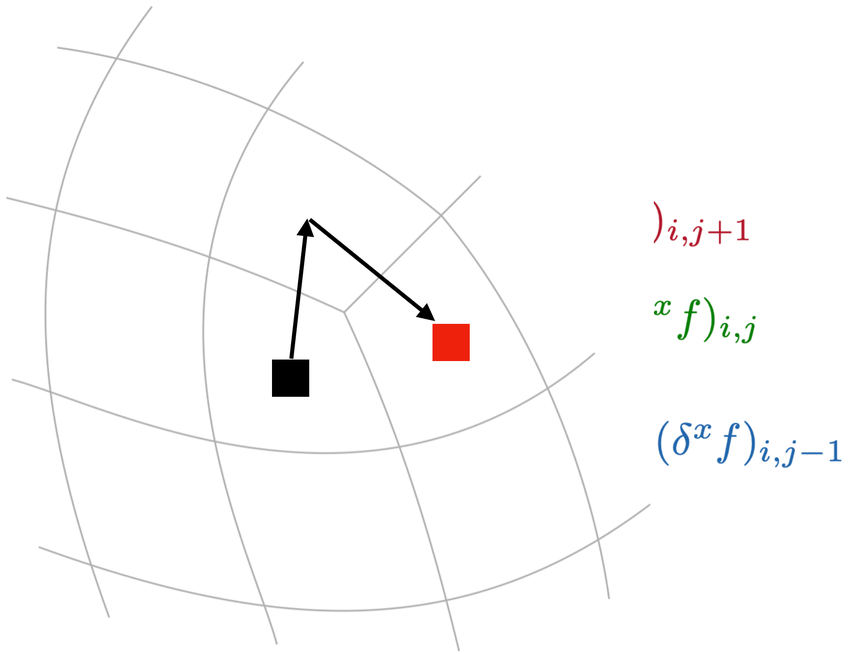
---

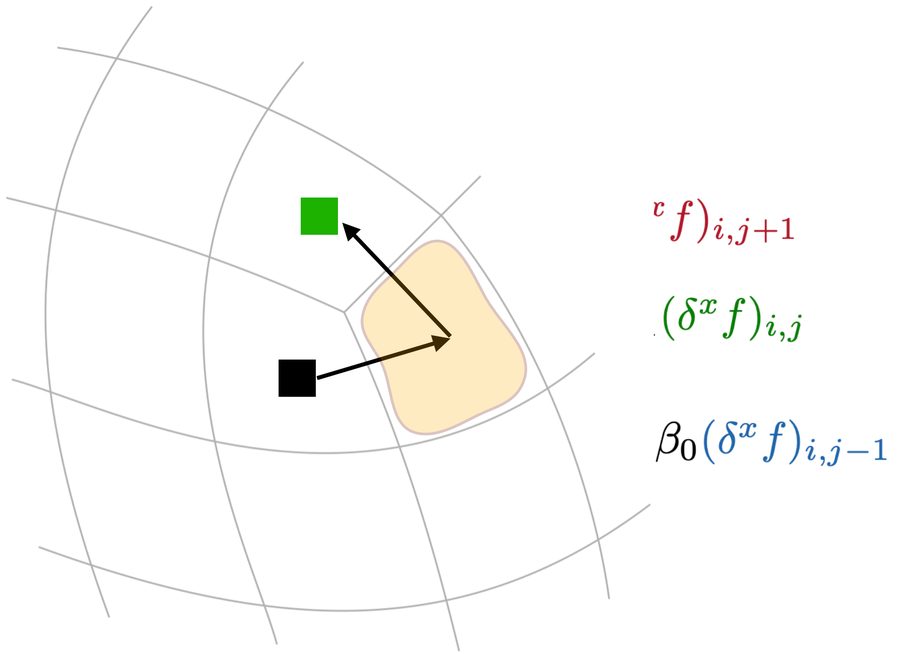
[1]. Deng et al. *Geometric conservation law and applications to high-order finite difference schemes with stationary grids*. JCP (2011).
[2]. Abe et al. *Geometric interpretations and spatial symmetry property of metrics in the conservative form for high-order finite derivative schemes...* . JCP (2014).

Geometric conservation law at grid singularities

Singularities introduce non-uniqueness

- Nested stencil operations are path dependent
- $(i, j) \rightarrow (i + 1, j + 1)$
- Schematically shown for 2nd order

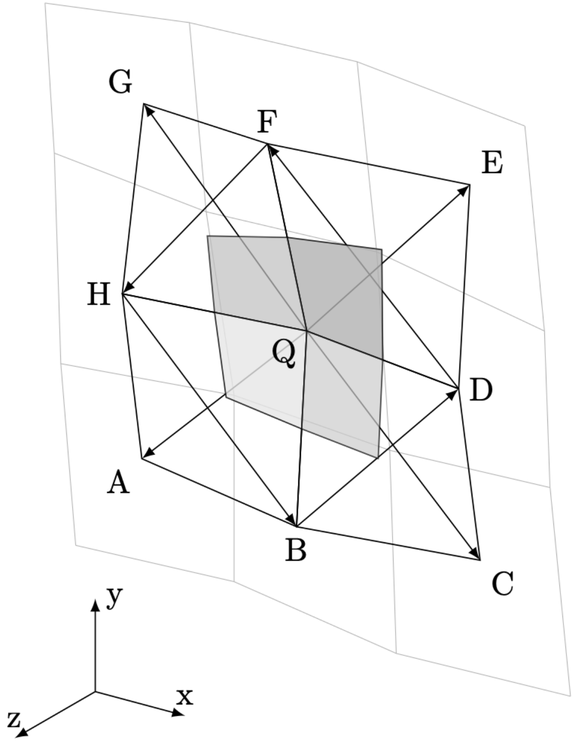




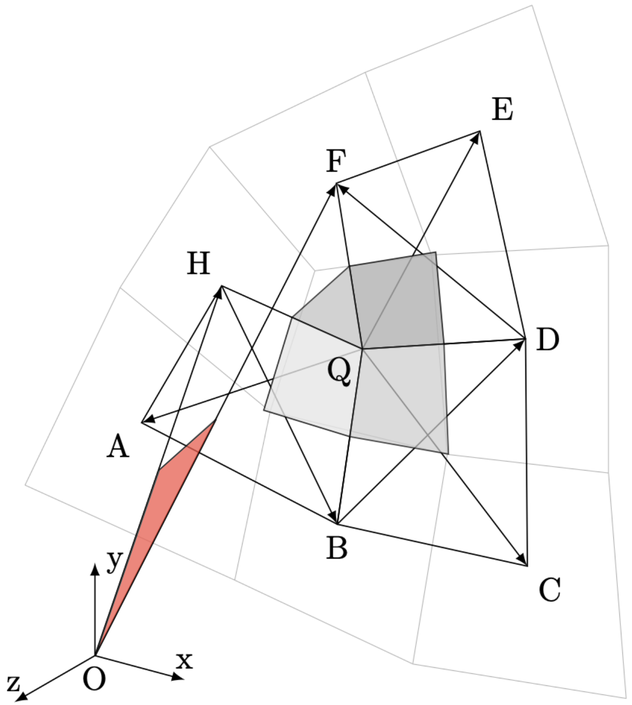
Geometrical interpretation

Metrics represent surface area vectors

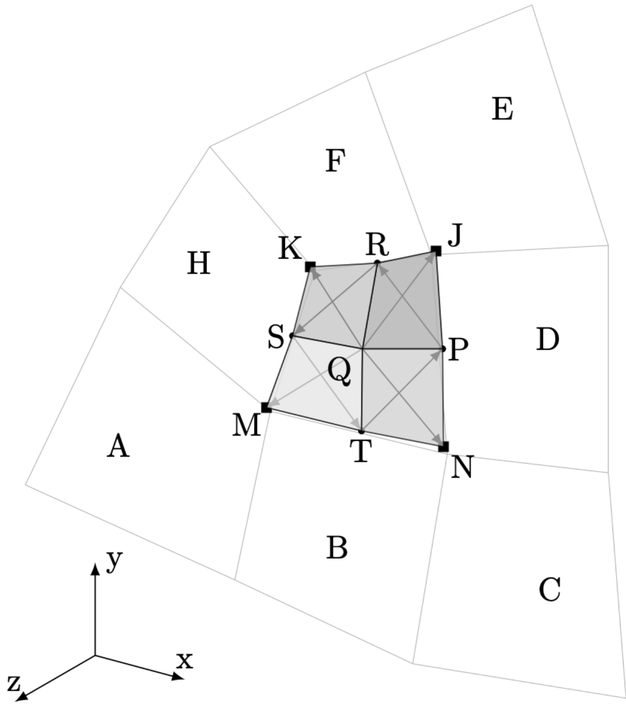
SCMM geometrically linked to actual grid



Single block grid



Multiblock collocated



Multiblock staggered

Proposed method A

Error at each grid point is $I_x\mathbf{F} + I_y\mathbf{G} + I_z\mathbf{H}$

Subtract the error as a source term[1]

$$\frac{\partial \widehat{\mathbf{C}}}{\partial t} + \frac{\partial \widehat{\mathbf{F}}}{\partial \xi} + \frac{\partial \widehat{\mathbf{G}}}{\partial \eta} + \frac{\partial \widehat{\mathbf{H}}}{\partial \zeta} - \frac{\partial \widehat{\mathbf{F}}_v}{\partial \xi} - \frac{\partial \widehat{\mathbf{G}}_v}{\partial \eta} - \frac{\partial \widehat{\mathbf{H}}_v}{\partial \zeta} = \dot{\widehat{\mathbf{S}}} + I_x\mathbf{F} + I_y\mathbf{G} + I_z\mathbf{H}$$

- Local (no stencil operations)
- Non-intrusive
- Non-conservative

[1]. Pulliam et al. *Implicit finite-difference simulations of three-dimensional compressible flow*. AIAA Journal (1980).

Proposed method B

Modify the reconstructed flux[1,2]

$$\left.\frac{\partial \widehat{\mathbf{F}}}{\partial \xi}\right|_{i,j,k} = \frac{1}{J}\left\{\left[\left(\mathbf{F}\xi_x\right)\Big|_{i+\frac{1}{2},j,k}\right] - \left[\left(\mathbf{F}\xi_x\right)\Big|_{i-\frac{1}{2},j,k}\right]\right\} + \cdots$$

$$\widetilde{\mathbf{F}}_{i+\frac{1}{2}} = \left(\widehat{\mathbf{F}}_{i+\frac{1}{2}} - \widehat{\mathbf{F}}^{c}_{i+\frac{1}{2}}\right) + \widehat{\mathbf{F}}^{c}_{i+\frac{1}{2}}$$

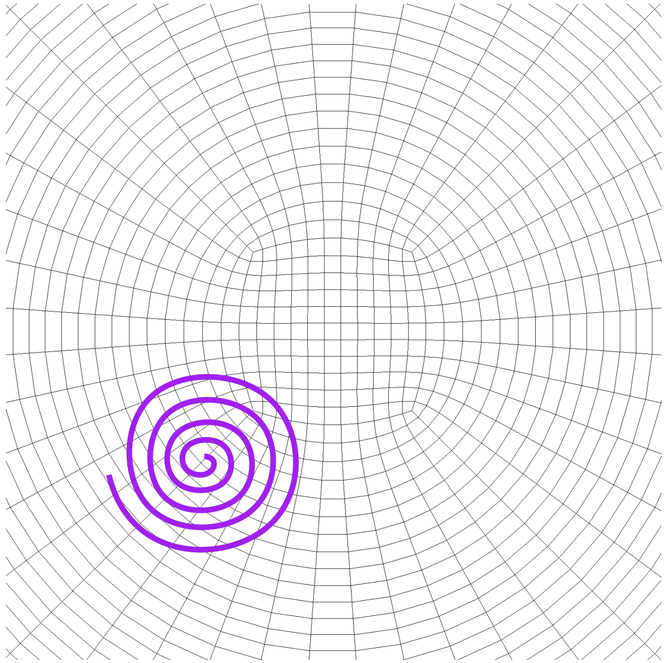
Default GCL

[1]. Zhu et al. *Free-stream preserving linear-upwind and WENO schemes on curvilinear grids*. JCP (2019).
[2]. Su et al. *Reformulated dissipation for the free-stream preserving of the conservative finite difference schemes on curvilinear grids*. JSC (2023).

Test cases

- Spatial symmetry
- Freestream preservation
- 2D vortex advection
- Poiseuille flow
- Acoustic modes in a pipe
- Radial shock tube
- Noh implosion
- 2D laminar flame speed
- Backward facing step
- Turbulent pipe flow (incompressible/compressible)

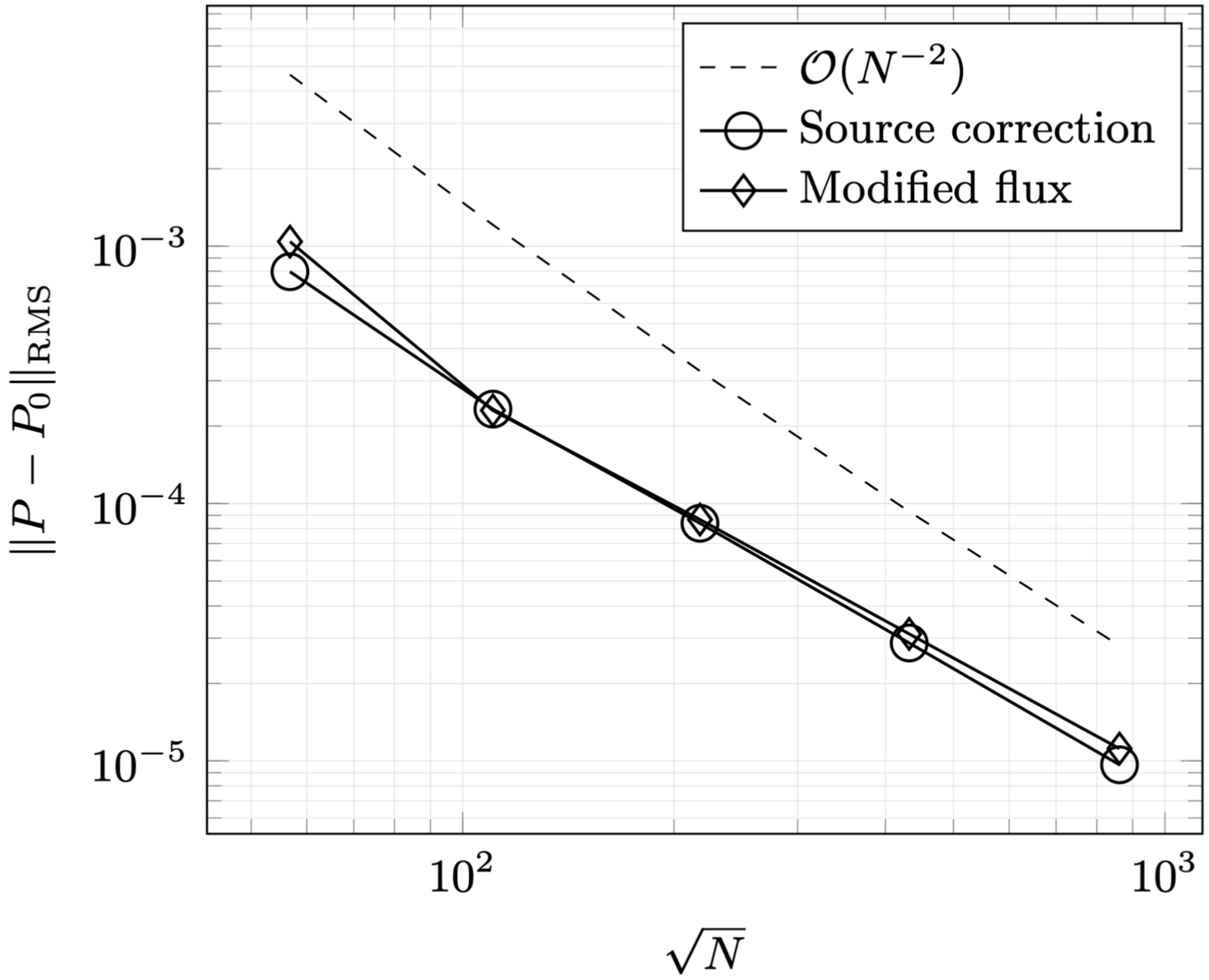
Isentropic vortex advection



$$\mathbf{u} = (0,1,1) + \mathbf{r} \times \left(0,0,-\frac{\beta}{2\pi}\sqrt{\exp\left(1-\mathbf{r}^2\right)}\right)$$

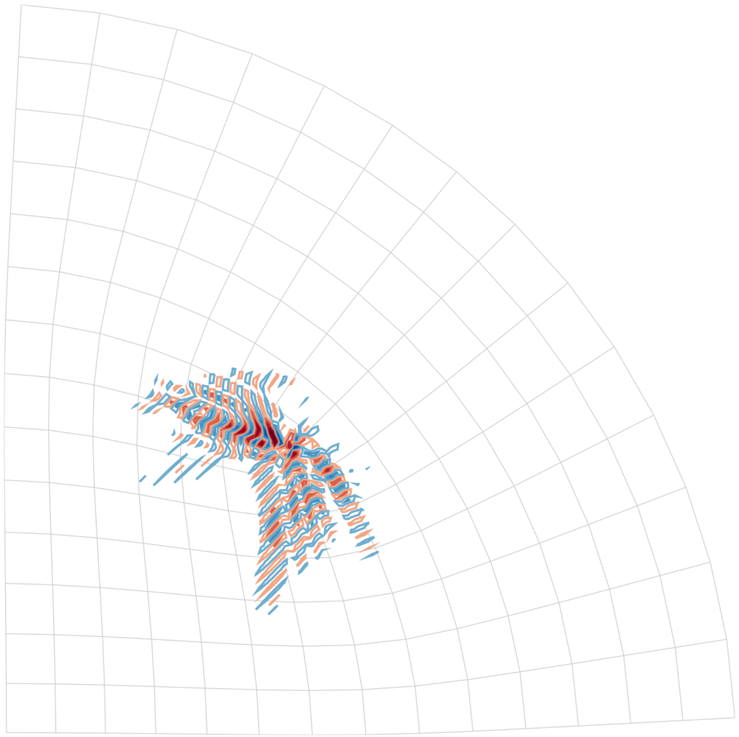
$$T = 1 - \frac{\gamma-1}{\gamma}\frac{\beta^2}{8\pi}\exp\left(1-\mathbf{r}^2\right)$$

$$P = T^{\frac{1}{\gamma-1}}$$

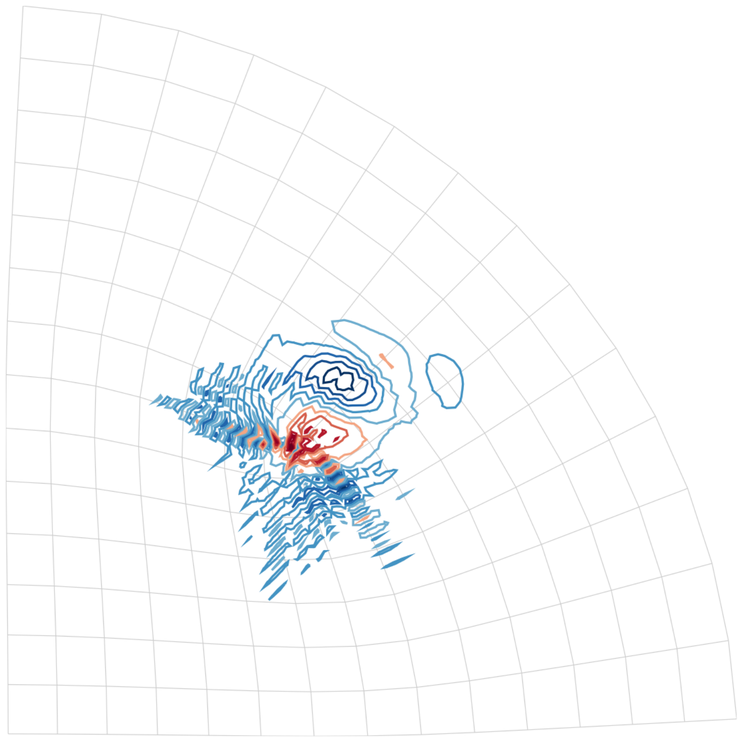


Isentropic vortex advection

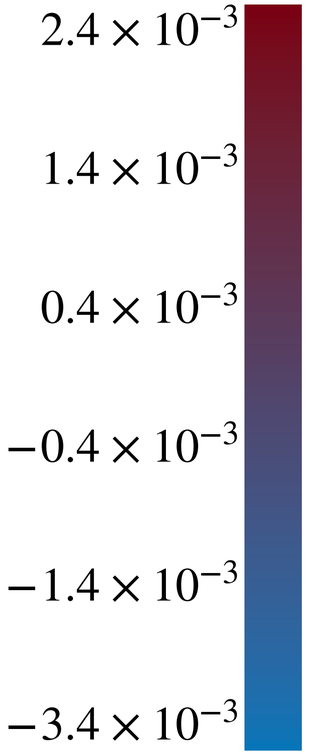
Pressure error contours: $(p - p_0)$



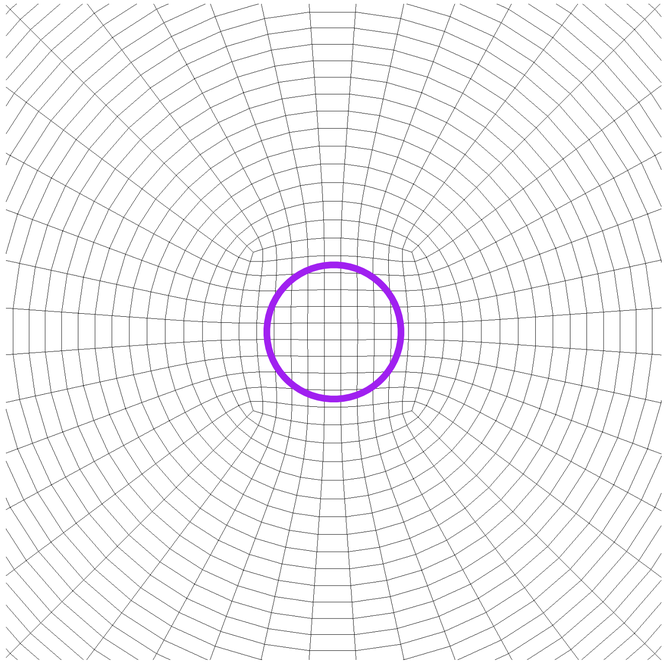
A: source correction



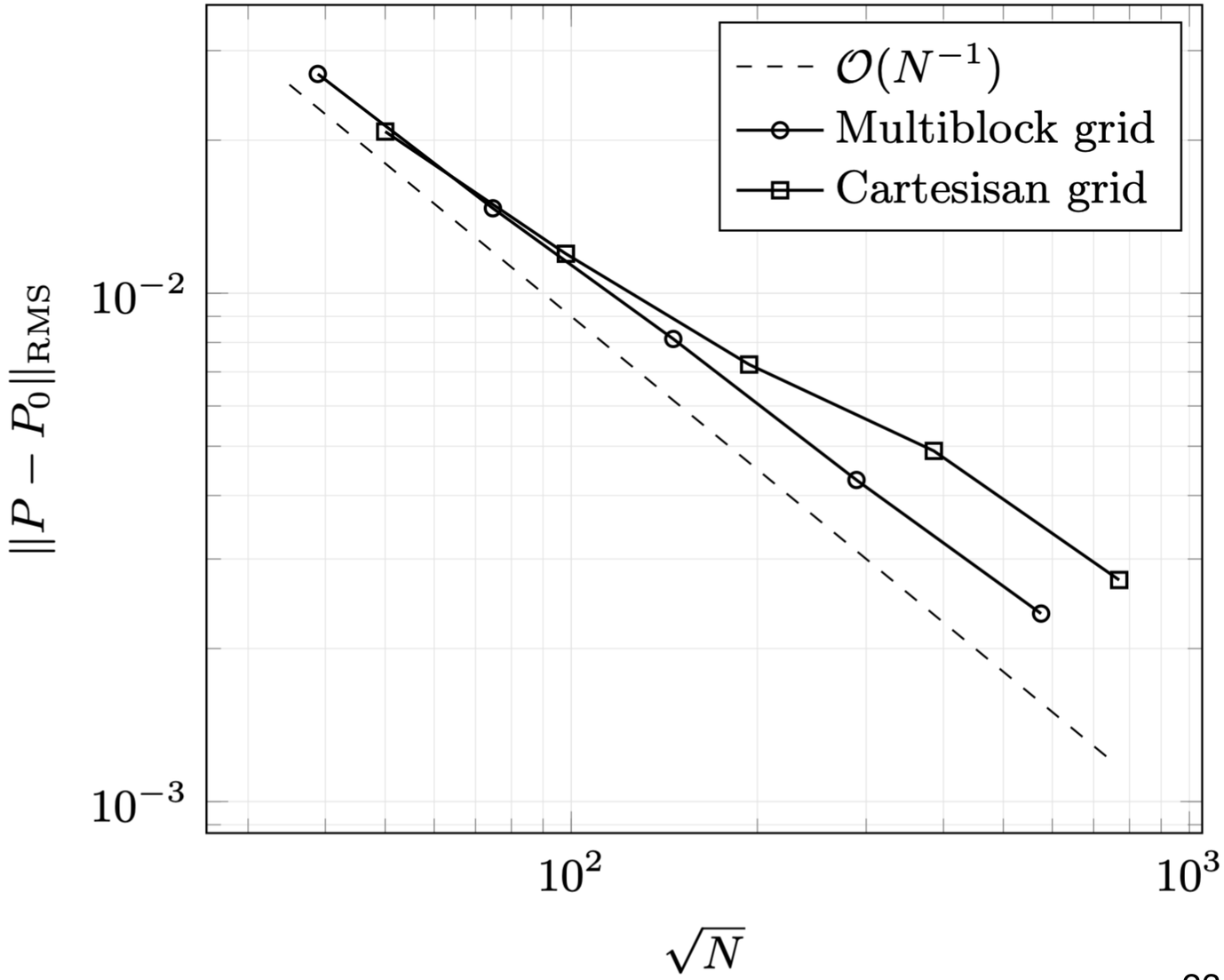
B: modified flux



2D Sod shock tube



$\mathbf{u} = 0.0$ $\quad$ $\mathbf{u} = 0.0$
$T = 1.0$, $\quad$ $T = 0.1$
$P = 1.0$ $\quad$ $P = 0.8$



Outline

- Introduction
- Effect of singularities on multiblock grids
- **Legion/Regent software stack**
- High Performance Computing
- Applications
- Conclusions

The Parallel Runtime Landscape

Chapel
[Chamberlain '07]

Legion/Regent
[Bauer '12, Slaughter '15]

IRIS
[Kim '21]

MPI

Parsec
[Bienia '08]

HPX
[Kaiser '14]

TBB
[Reinders '07]

Charm++
[Kale '93]

Cilk/Cilk++
[Blumofe '95]

Legion runtime

Task-based

- Dynamic task graph
- Distributed parallel scheduling

Advantages of data awareness

- Partitioning
- Communication patterns
- Synchronisation

```
task do_work( fluid : region(fields),
              ghost : region(fields))
where
   reads(fluid.rho, ghost.rho),
   writes(fluids.rhs)
do
   ...
end
```

Regions

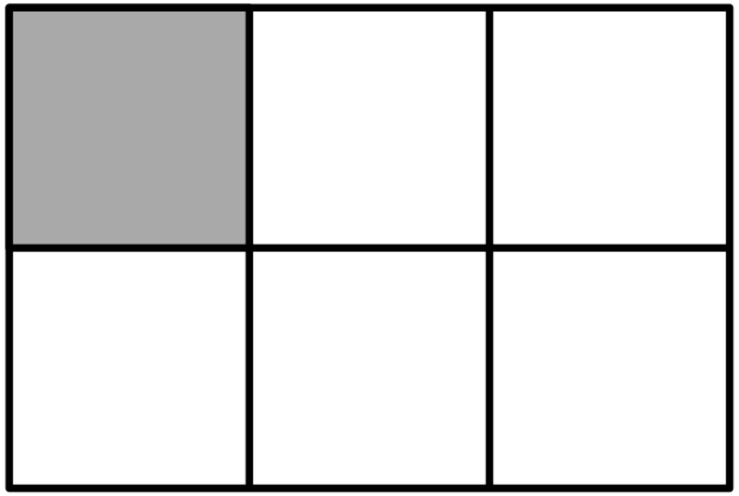
Core data containers in Legion

Index space (where) x Field space (what)

Sub-regions: partitions in logical space

Data accessors

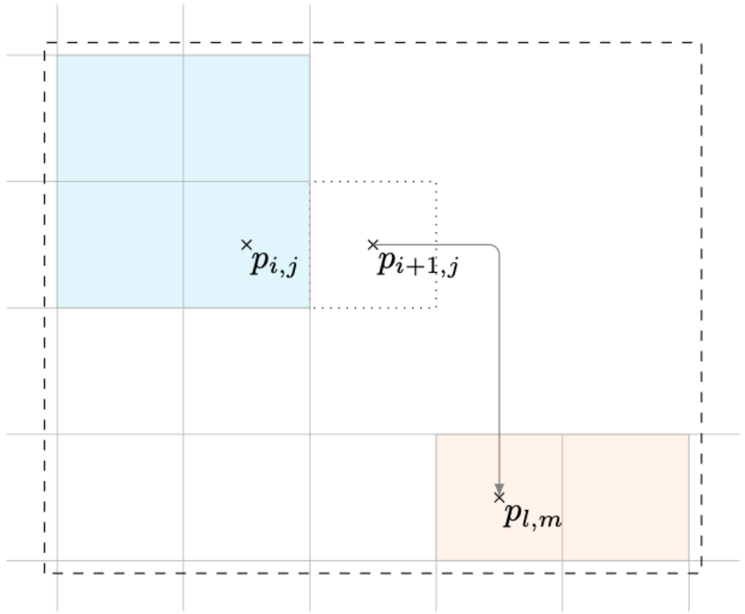
- Affine
- Multi-affine



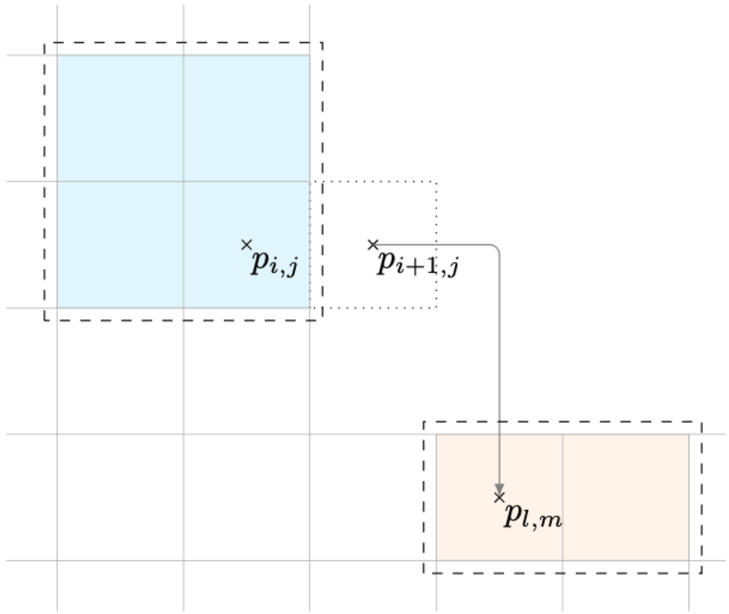
Data accessors

Stencils span multiple blocks

Logical space .vs. Memory layout



Affine accessors:
fast but memory intensive

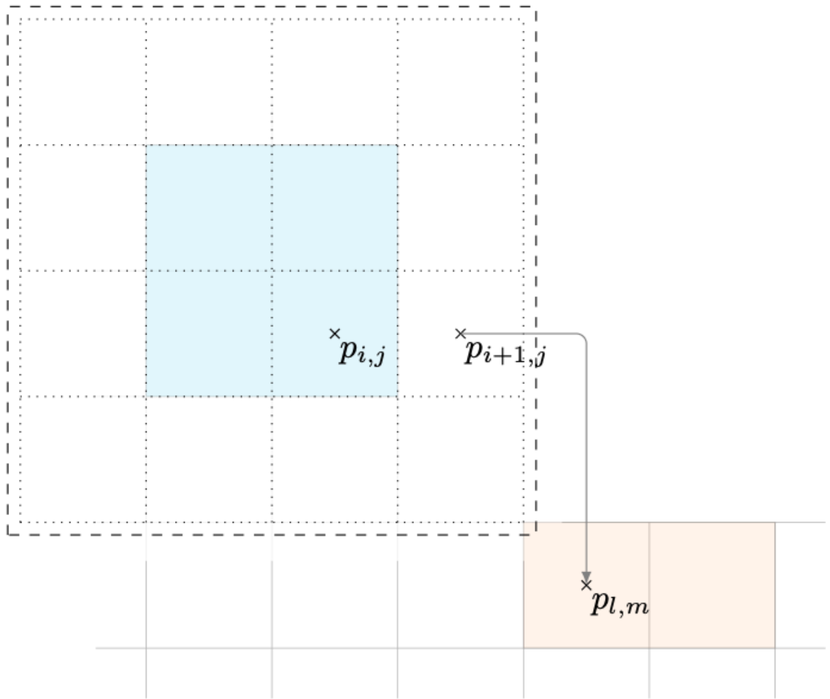


Multiaffine accessors:
slow but memory efficient

Padded instances

Exploit separation between logical views and memory allocation

- Manageable memory footprint
- Efficient



Partitioning and mapping

Partitioning

- Load balancing algorithm
- No-large-outlier policy
- General arbitrary topologies

Mapping

- Minimizing network traffic

User	Legion
Partitioning	Data dependency map
Mapping	Inter-partition communication
	Memory allocation
	Data transposition

Performance figures on LLNL Lassen

Profiling for the convective flux kernel

Accessor	**Total** [ms]	**Data assembly** [ms]	**Compute** [ms]	**Memory** [%]
Affine	31	N/A	31	300
Multi-affine	42	N/A	42	100
Padded	25	3	22	102

Performance penalty

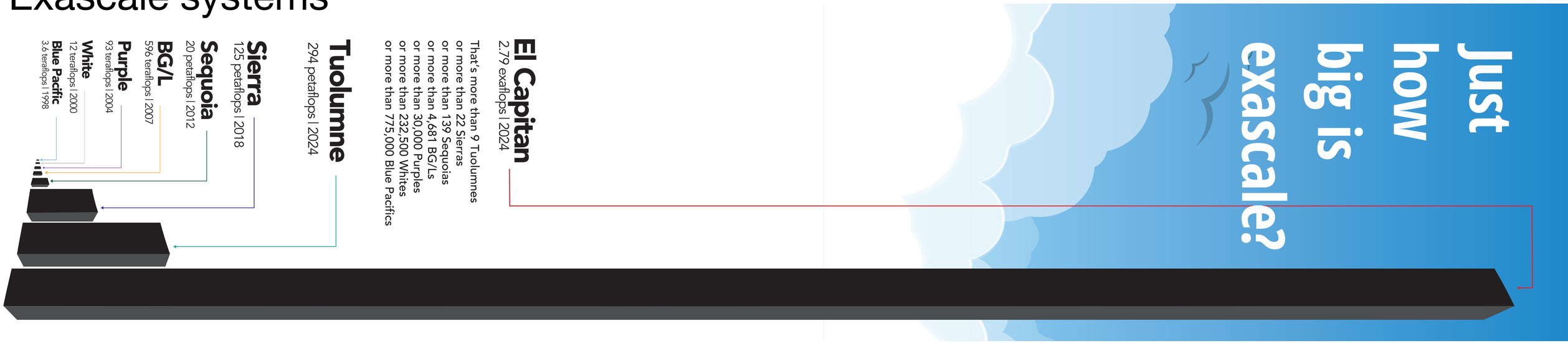
Grid size	**Slowdown factor**
200^3	1.5
238^3	1.44
225^3	1.18

Outline

- Introduction
- Effect of singularities on multiblock grids
- Legion/Regent software stack
- **High Performance Computing**
- Applications
- Conclusions

Computing facilities

Exascale systems



System size ∝ Complexity

HTR: general, multi-physics solver

- Top → down algorithmic approach

What is possible to achieve?

---

[1]. Lawrence Livermore National Lab. https://asc.llnl.gov/exascale/el-capitan.

State of the art

Scaling results *[**HTR**: Di Renzo '20, **STREAmS**: Bernardini '21, **PadeLibs**: Song '22, **SU2**: Economon '15, **Alya**: Vazquez '16, **SPARC**: Howard '17, **...**]*

- Weak scaling
- Strong scaling

Achieved fraction of absolute peak performance

- 5% *[Cameron '05, Decyk '96]*
- 13% *[Fu '23]*

Kernel specific reports

- Hand tuned *[Li '18, Compack3D '25]*
- Compiler directives & Metaprogramming *[**Uranos**: De Vanna '24, **MFC**: Bryngelson '21,'24]*

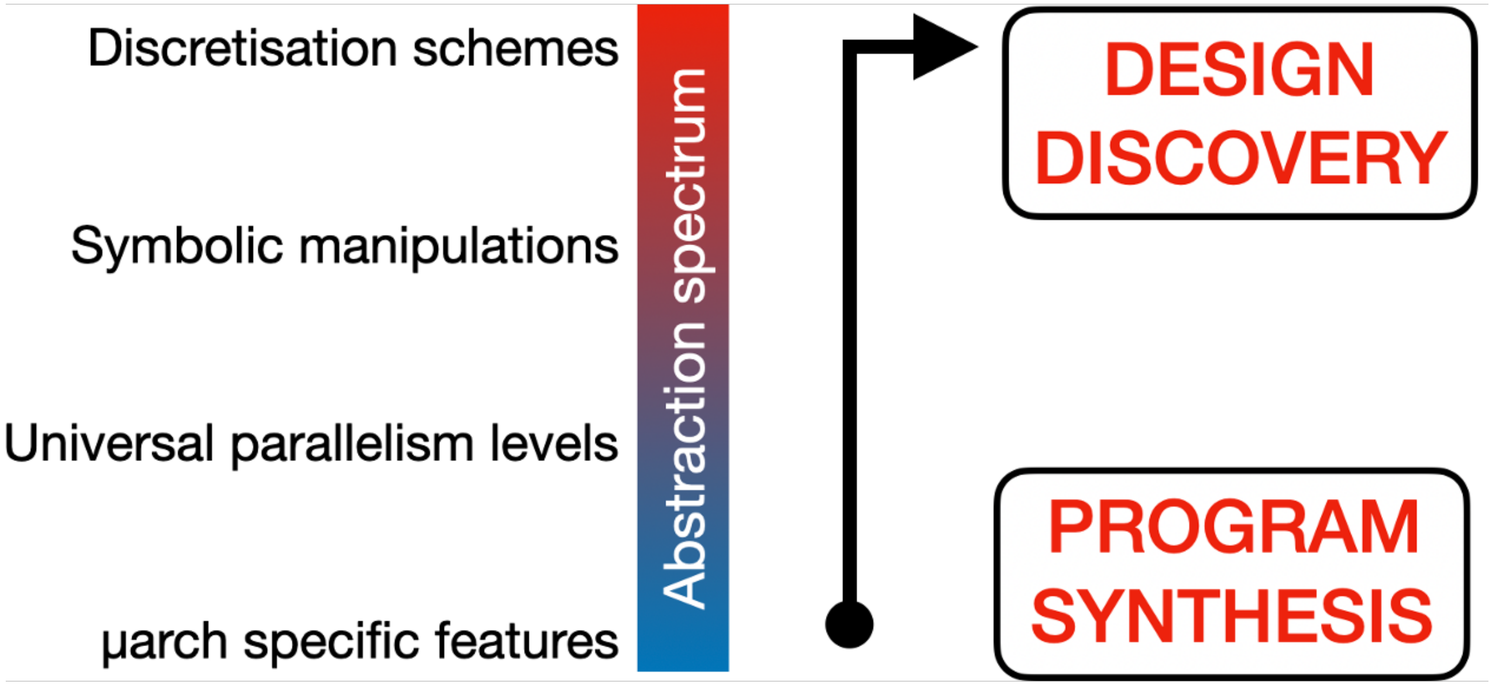
Systematic approach to performance

Start with the hardware

- Small, synthetic microbenchmarks[1]
- Timescales
- Attainable limits

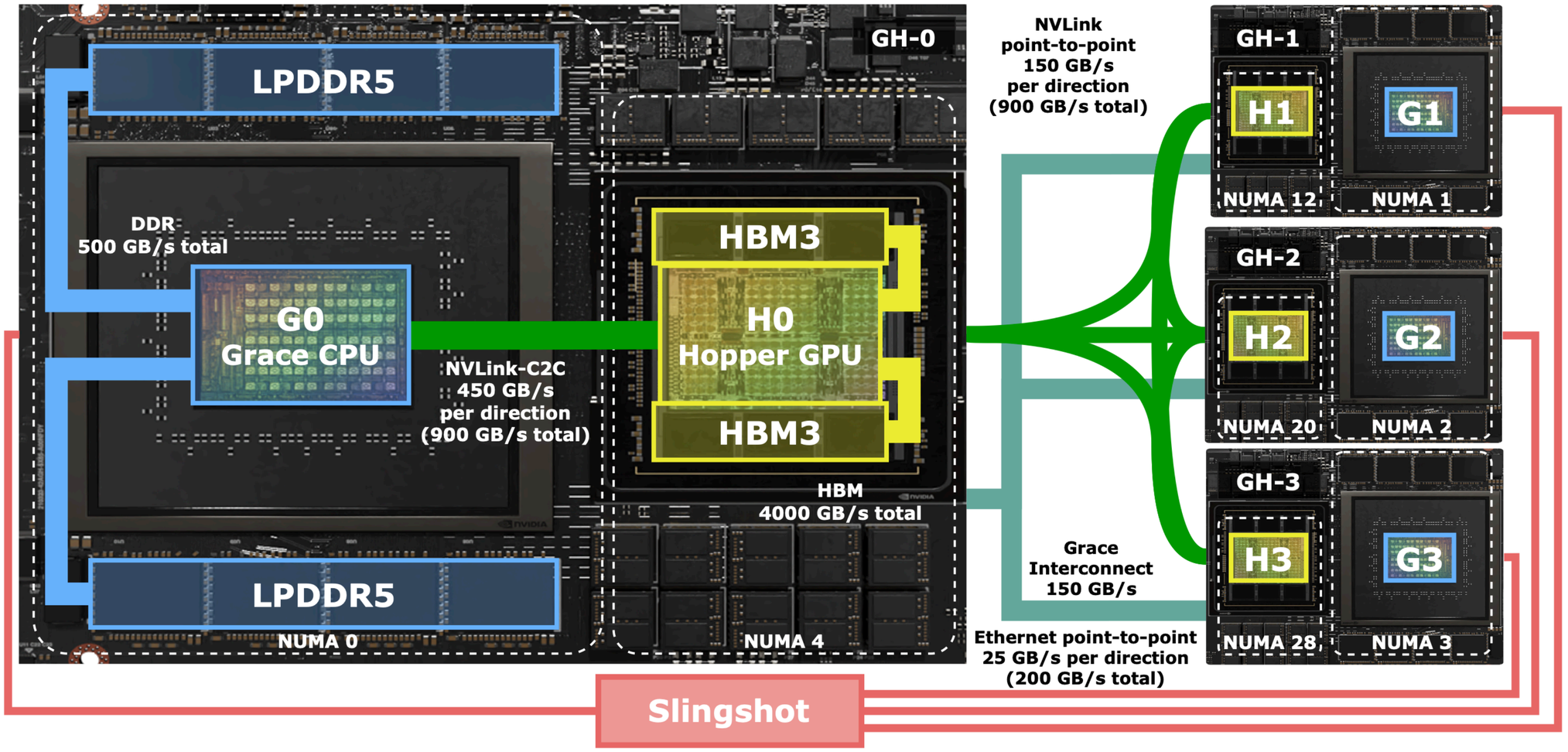
Build bottom→up

- Discover by measuring



[1]. STREAM, mpiBench, OSU, Nvbandwidth

Levels of parallelism and time scales

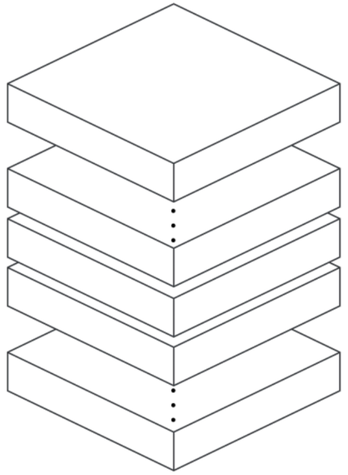


[1]. Fusco et al. *Understanding data movement in tightly coupled heterogeneous systems: A case study with the Grace Hopper superchip*. arXiv preprint (2024).

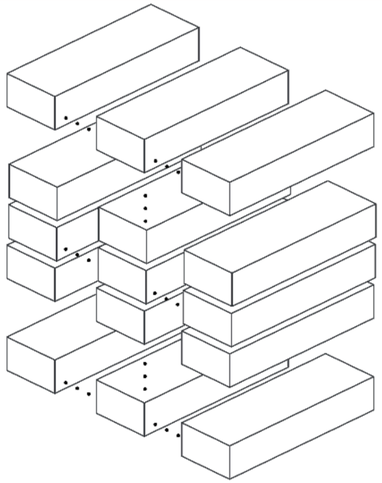
Domain decomposition

Working regime

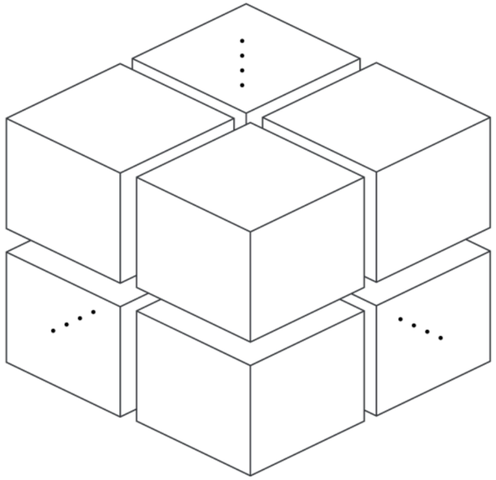
- Network
- Bandwidth
- Compute



Slab ——

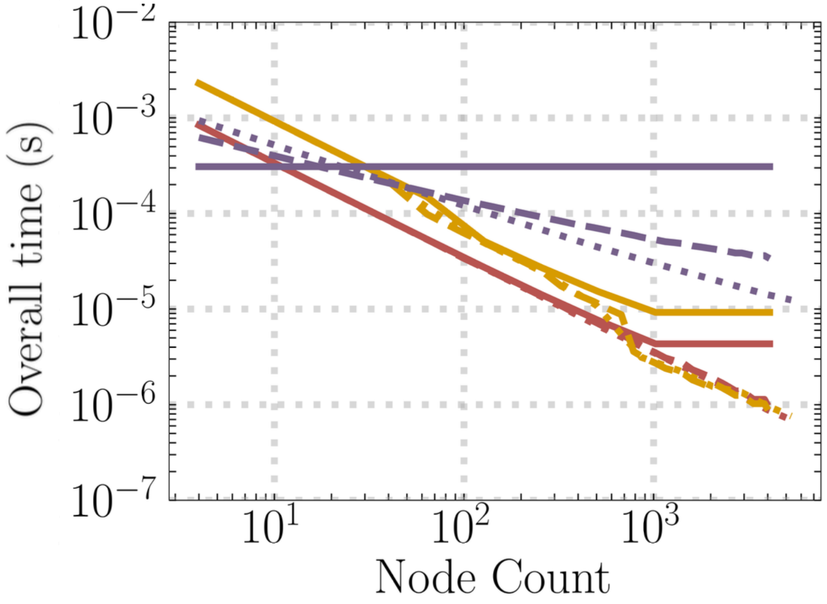


Pencil ----

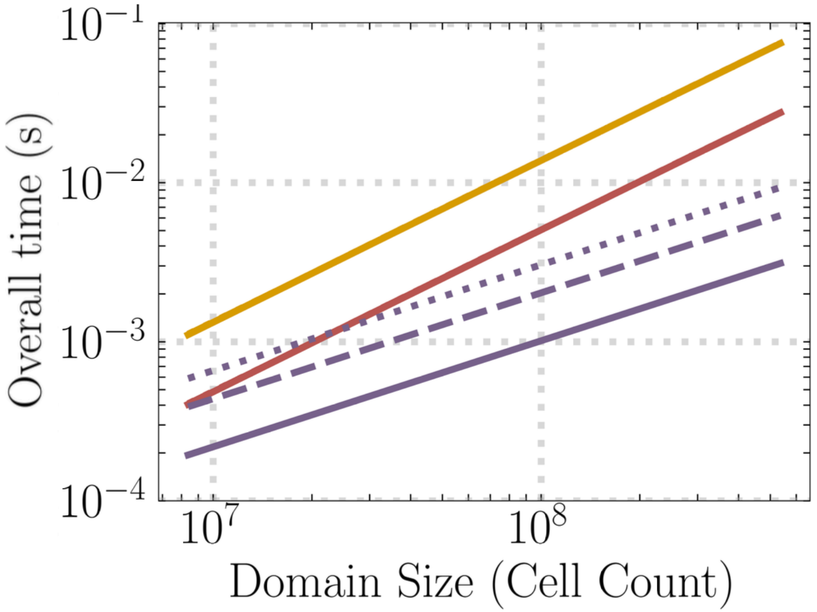


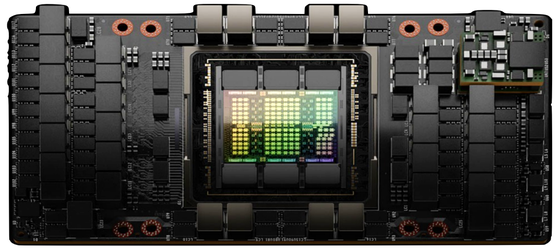
Cube ⋯⋯

Strong scaling



Weak scaling





NVIDIA H100 GPU

Kernel synthesis

Symbolic framework[1]

- High performance code is not human friendly

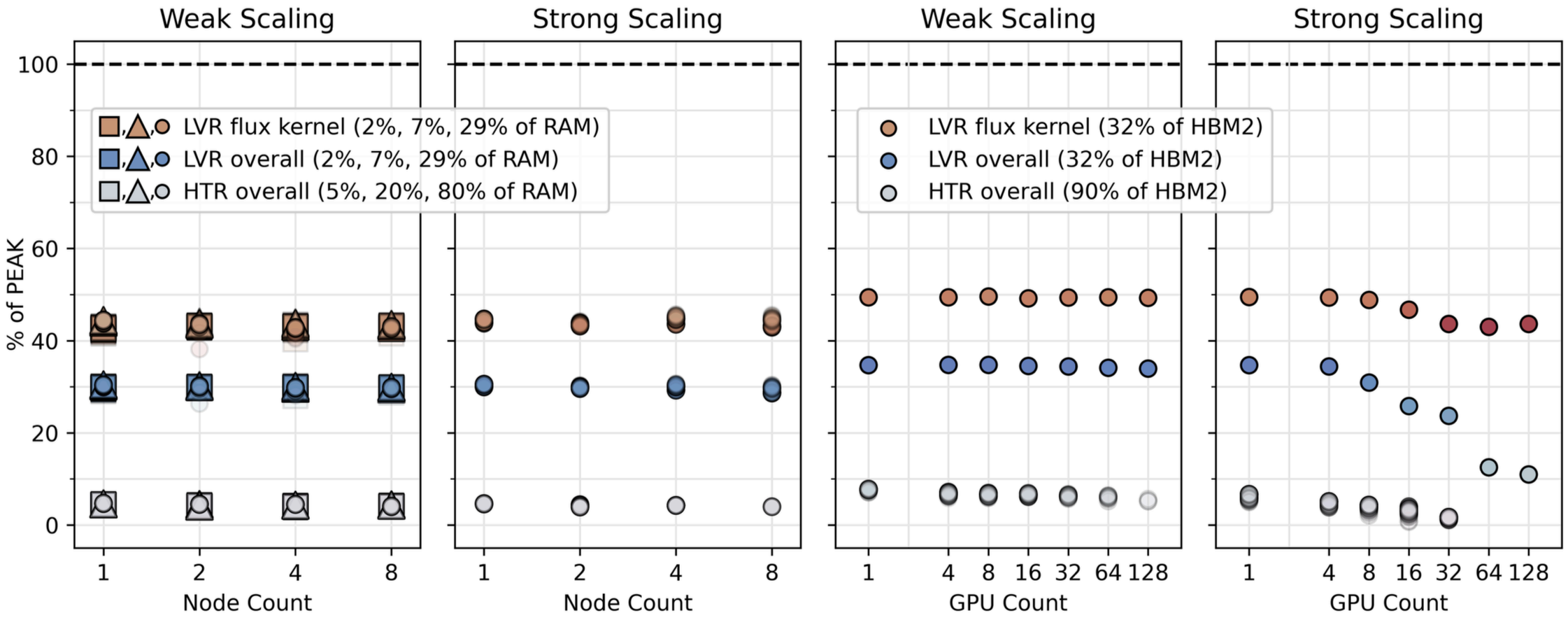
```
const double x114 = 6*1.0/(x107 + x112)*1.0/(10*x107 + x113);
const double x115 = x47 - x48;
const double x116 = (x11 - x40 + x41 - x42 + x44)*(x115 + x45);
const double x117 = -x57;
const double x118 = (x115 + x117 + x5 + x55 + x56)*(-x59 + x6);
const double x119 = 1.0/(WENOEPS + x116 + x118)*1.0/(10*x116);
const double x120 = -x70;
const double x121 = x120 + x72;
const double x122 = (0.125*p_m1[i] + 0.375*p_p1[i] - x108 - x121);
const double x123 = -x5;
const double x124 = (0.54166666666666663*p_m1[i] + 0.5416666666666
const double x125 = WENOEPS + x124;
const double x126 = 10*x124 + x36;
const double x127 = 3*1.0/(x122 + x125)*1.0/(10*x122 + x126);
const double x128 = 1.0/(x114 + x119 + x127);
```

```
s_load_dwordx4 s[0:3], s[4:5], 0x68
v_fmac_f64_e32 v[26:27], v[4:5], v[10:11]
v_mul_f64 v[26:27], v[22:23], v[26:27]
v_fmac_f64_e32 v[26:27], v[42:43], v[30:31]
v_mov_b32_e32 v31, s19
v_add_co_u32_e32 v30, vcc, s18, v0
v_mul_f64 v[10:11], v[28:29], v[20:21]
v_addc_co_u32_e32 v31, vcc, v31, v1, vcc
v_mul_f64 v[20:21], v[46:47], v[20:21]
global_store_dwordx2 v[30:31], v[26:27], off
v_mul_f64 v[26:27], v[40:41], v[24:25]
v_mul_f64 v[24:25], v[52:53], v[24:25]
v_fmac_f64_e32 v[10:11], v[4:5], v[20:21]
v_fmac_f64_e32 v[26:27], v[14:15], v[24:25]
v_mul_f64 v[10:11], v[22:23], v[10:11]
```

[1]. Meurer et al. *SymPy: symbolic computing in Python*. PeerJ Computer Science (2017).

Results

Comparisons with HTR



(a) 2× Intel Xeon Platinum 8480+ **(b) NVIDIA V100 SXM2**

Results

Portability on different machines

Machine	Processor	% of Peak
Lassen LLNL	NVIDIA Tesla V100 SXM2	35
Dane LLNL	Intel Xeon Platinum 8480+	32
Aurora ALCF	Intel Data Center Max 1550 Series (Ponte Vecchio)	25
Aurora ALCF	Intel Xeon CPU Max 9470	29
Alps CSCS	NVIDIA H100 Hopper	38
Alps CSCS	NVIDIA Grace Superchip	25
Odyssey Frank UO	AMD Instinct MI300A	33

Outline

- Introduction
- Effect of singularities on multiblock grids
- Legion/Regent software stack
- High Performance Computing
- **Applications**
- Conclusions

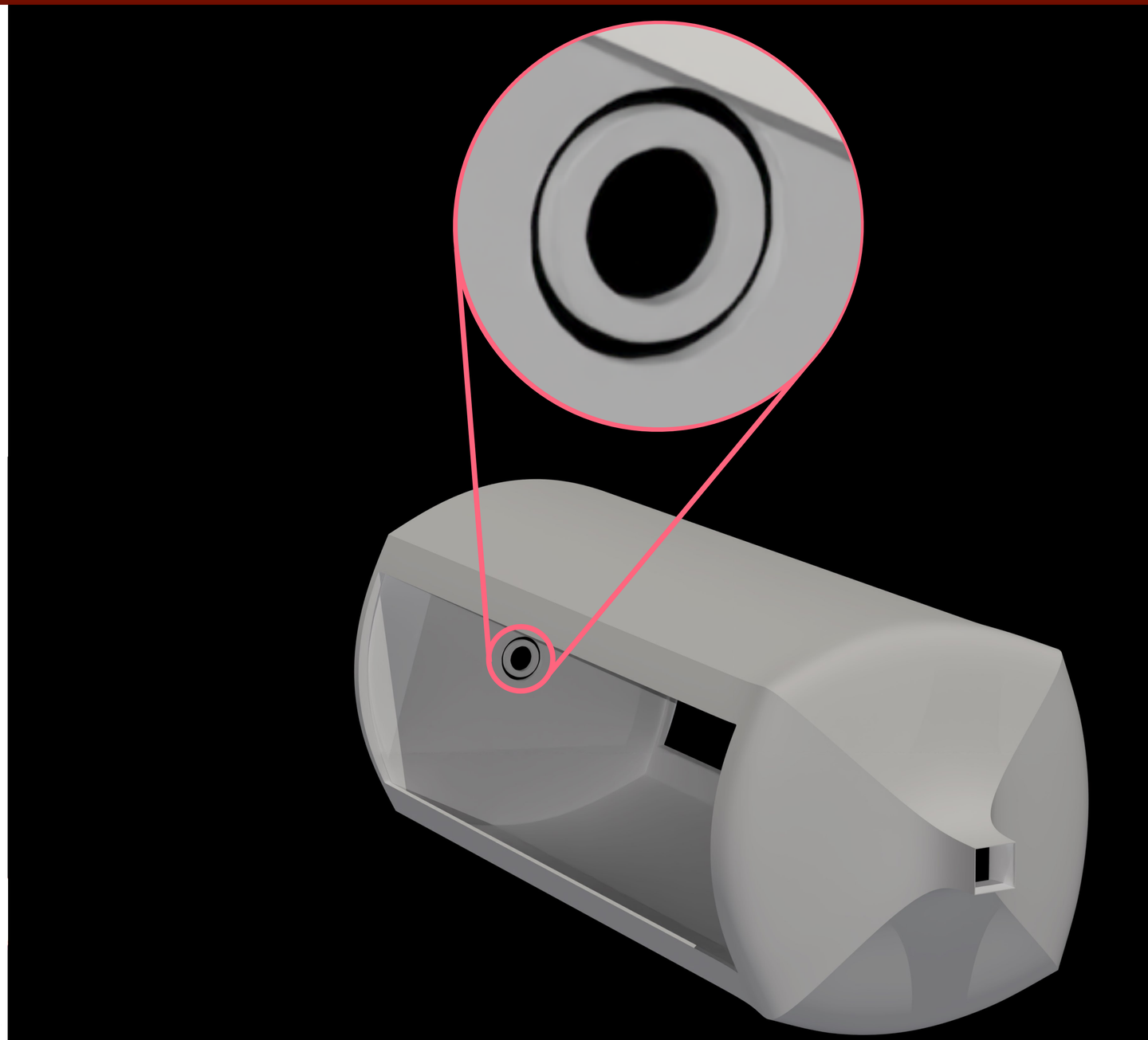
Integrated simulations

Advance the current state of the art

- Turbulent multicomponent mixing
- Reacting flow
- Simplified geometry
- Multiphase capabilities

Problem description:

- Methane co-flow
- Oxygen



[1]. Brouzet et al. CAF (2026).

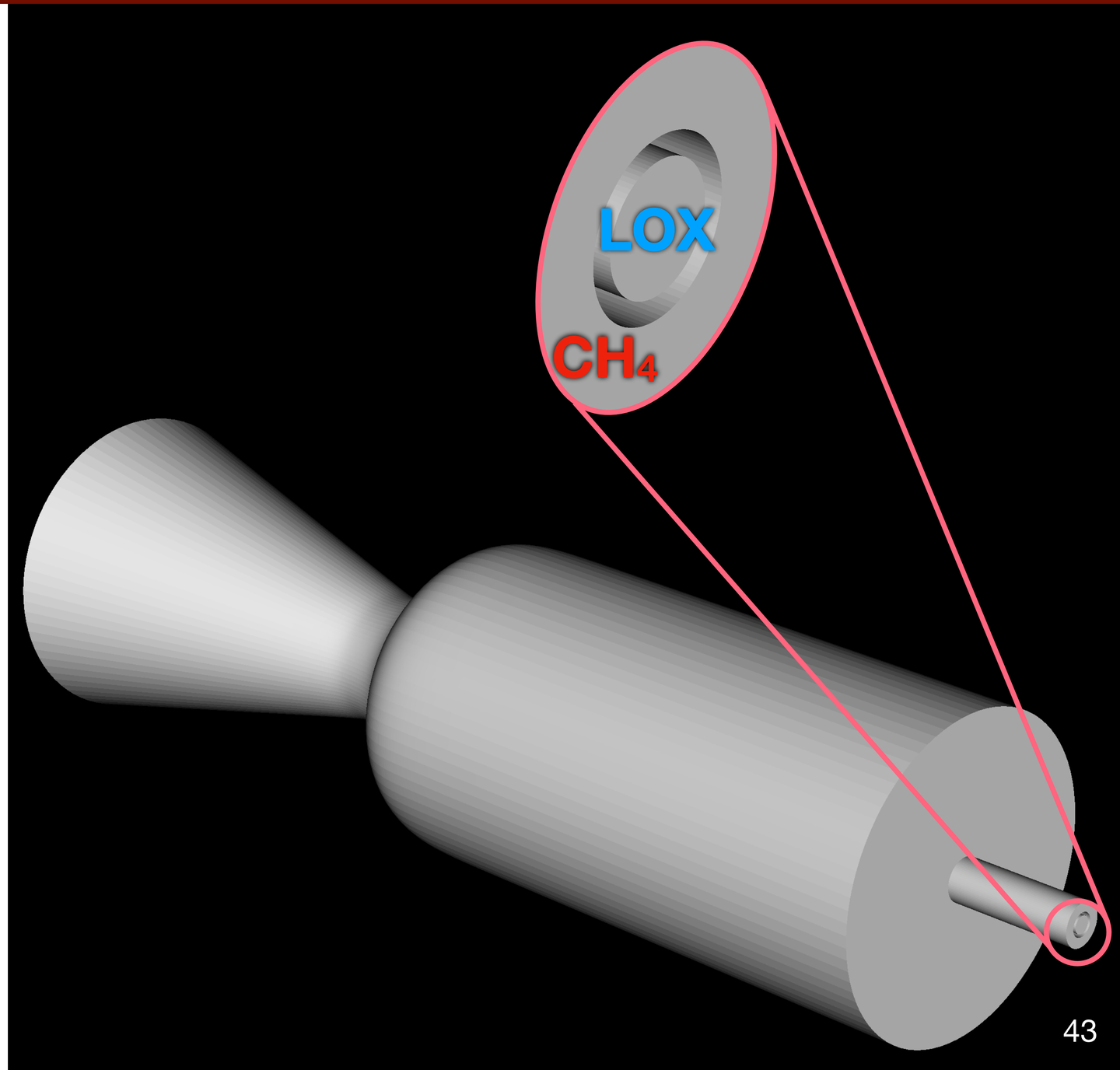
Integrated simulations

Advance the current state of the art

- Turbulent multicomponent mixing
- Reacting flow
- **Realistic geometry**
- Multiphase capabilities

Problem description:

- Methane co-flow at 260 K and 37 kPa
- **Liquid** oxygen at 100 K and at 145 kPa
- Low pressure exhaust at 7 kPa



Integrated simulations

Problem description:

- Choked methane co-flow at 260 K and 37 kPa
- Choked liquid oxygen at 100 K and at 145 kPa
- Low pressure exhaust at 7 kPa

IGNITION

16 Species Reacting

T=900 K

TEMPERATURE

HIGH

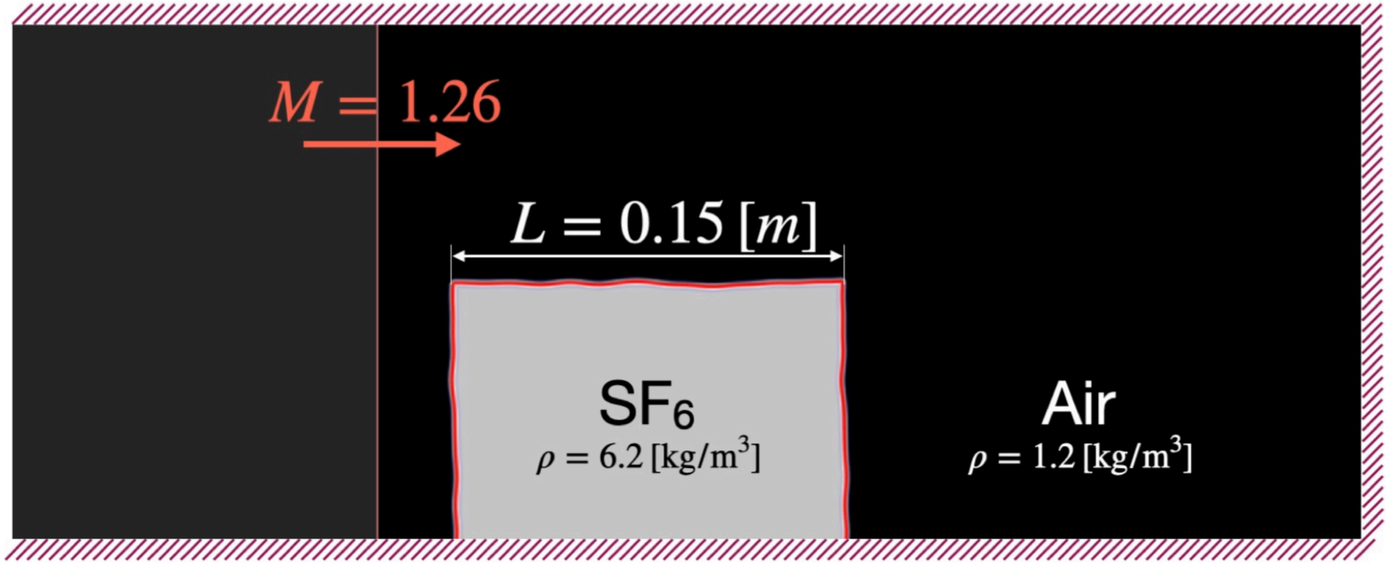
LOW



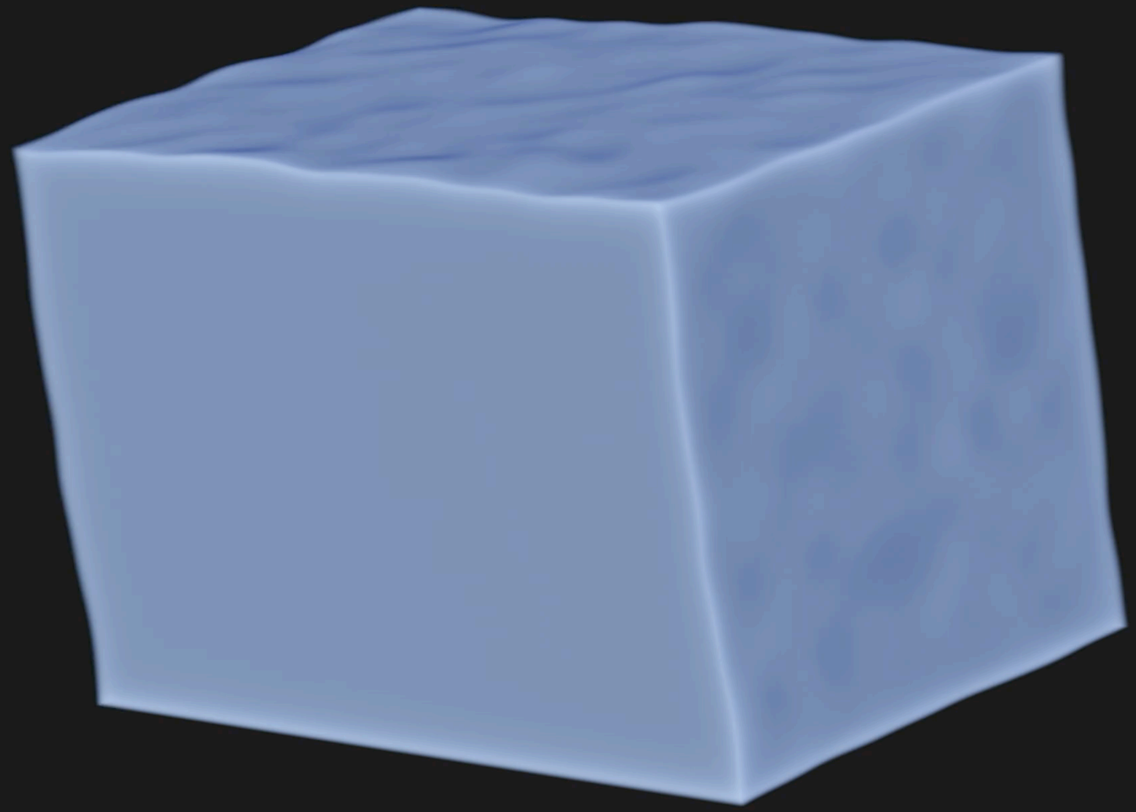
Integrated simulations

Problem description:

- Rectangular SF6 block in air
- Thermal and mechanical equilibrium
- Incoming $M = 1.26$ shock wave



DENSITY MAGNITUDE



VORTICITY MAGNITUDE

Outline

- Introduction
- Effect of singularities on multiblock grids
- Legion/Regent software stack
- High Performance Computing
- Applications
- **Conclusions**

Conclusions

Numerical framework for DNS/LES with multiblock structured grids

- Methods to mitigate the effects of grid singularities and restore GCL
- Improve the performance of the HTR solver by 60-100% through padded instances

Introduced a methodology for building HPC solvers

- Bottom-up approach
- Measurable absolute performance

Integrated liquid rocket combustor

- Comparable results with experiments
- Predictive LES results to refine experimental measurement protocols
- Explored uncertainty areas in regions where experimental measurements are impossible

Relevant publications

In preparation:

- **Voci, A.**, Di Renzo, M., Lele, S. & Iaccarino, G. *A distributed multiblock solver for compressible flows using the Legion runtime*.
- **Voci, A.**, Grinstein, F., Chiravalle, V.P. & Lele, S. *Detailed statistical analysis of half-height shock tube problem*.
- Trabacchin, T., **Voci, A.**, Collis, H., Khanwale, M., Zahtila, T., Zulian, P., Brouzet, D., Iaccarino, G. & Rossinelli, D. *Boosting CFD to 50% of Peak on Exascale Systems*.

Published:

- Brouzet, D., Rossinelli, D., Zahtila, T., **Voci, A**., Strelau, R., Warner, A., Gejji, R., Slabaugh, C., & Iaccarino, G. *Thermal expansion-driven laser ignition in a gas subscale rocket combustor*. Combustion and Flame (2026).
- **Voci, A.**, Collis, H., Zahtila, T., Brouzet, D. J., Rossinelli, D., Mani, A., Lele, S. & Iaccarino, G. *Multi-fidelity Data Ensembles of Liquid Phase Rocket Ignition: Ignition Limit States and Reliability*. AIAA SCITECH Forum (2026).
- Rossinelli, D., Trabacchin, T., **Voci, A.**, Brown, L., Collis, H., Khanwale, M., Zahtila, T., Brouzet, D. & Iaccarino, G. *Crafting software in HPC: a quantitative approach*. Center for Turbulence Research Annual Research Briefs (2025).
- Rossinelli, D., Li, G., **Voci, A.**, Marshall Jr., L., Hu, J., Brouzet, D., Fan, T., Williams, C., Martin, O., Khanwale, M., Vignat, G., Zahtila, T., Cutforth, M. & G. Iaccarino. *High-fidelity modeling of shadowgraphy and schlieren imaging*. Center for Turbulence Research Annual Research Briefs (2025).
- **Voci, A.**, Grinstein, F., Chiravalle, V.P., Regele, J.D. & Lele, S.K. *High-resolution simulations of transitional triple point shock interactions*. LA-UR-21-30418 (2021).